

Supplementary Information

Water Transport in Polymer Composites through Swelling-Induced Networks of Hydrogel Particles

Johannes Eiler^{1,2}, Søren Bredmose Simonsen³, Daniel Hansen^{1,2}, Bahar Bingöl², Kristoffer Hansen², and Esben Thormann^{*1}

¹Department of Chemistry, Technical University of Denmark, 2800 Kgs. Lyngby, Denmark

²Coloplast A/S, 3050 Humlebæk, Denmark

³Department of Energy Conversion and Storage, Technical University of Denmark, 2800 Kgs. Lyngby, Denmark

*Corresponding author: esth@kemi.dtu.dk

1 Model Calculations for the Interparticle Distance

To estimate the spacing between the particles within the composite, a simple model with spheres in a hexagonal close-packed (hcp) structure was established. The unit cell is a hexagonal prism, which contains six complete spheres (see Fig. S1 a). Its volume, V_{hcp} , can therefore be expressed as a function of the radius of the particle, r , and the particle volume fraction, ϕ :

$$V_{hcp} = \frac{6}{\phi} \cdot \frac{4}{3\pi} \cdot r^3 \quad (1)$$

The unit cell has a basal side length, a , and a height, h , which corresponds to the height of two tetrahedra with side length a :

$$h = 2 \cdot \frac{\sqrt{6}}{3} \cdot a \quad (2)$$

The volume of the unit cell can therefore also be written as:

$$V_{hcp} = \frac{3\sqrt{3}}{2} \cdot a^2 \cdot h = \frac{6}{\sqrt{2}} \cdot a^3 \quad (3)$$

Through Eq. 1 and 3, the basal side length can be expressed as:

$$a = \left(\frac{\sqrt{2}}{\phi} \cdot \frac{4\pi}{3} \right)^{\frac{1}{3}} \cdot r \quad (4)$$

In the model, the interparticle distance, δ_{model} , is calculated as the distance between the surfaces of two neighbouring spheres:

$$\delta_{model} = a - 2r = \left(\left(\frac{\sqrt{2}}{\phi} \cdot \frac{4\pi}{3} \right)^{\frac{1}{3}} - 2 \right) \cdot r \quad (5)$$

The resulting interparticle distances are shown as a function of particle loading and particle size in Fig. S1 b.

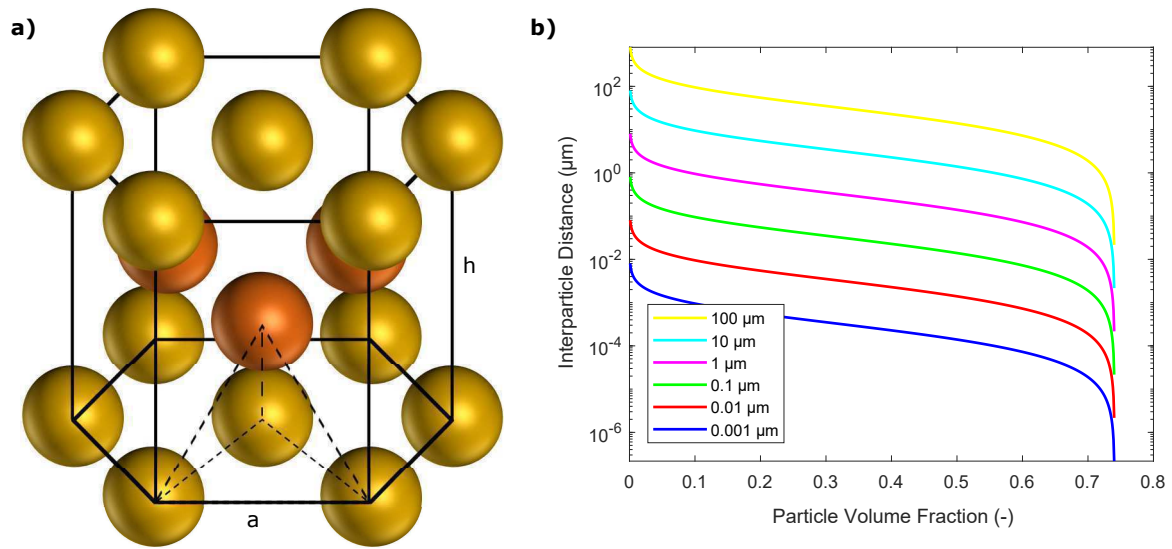


Figure S1: a) In the theoretical model, spherical particles were arranged in a hexagonally close-packed structure. The size of the spheres and the unit cell were determined by the particle size and their volume fraction respectively. b) The resulting interparticle distance, δ_{hcp} , as a function of particle volume fraction, ϕ , for different particle diameters.

2 Structural Analysis

X-ray μ CT measurements were conducted to evaluate the internal structure of the polymer composites at nominal particle loadings, ϕ_{nom} , of 0.09, 0.12, and 0.27. An example of the data obtained from the measurements is shown in Fig. S2 a and b. The individual hydrogel particles were segmented out and visualised within the polymer matrix and compared to the morphology of the hydrogel particles before incorporation into the polymer matrix (see Fig. S3 a and b).

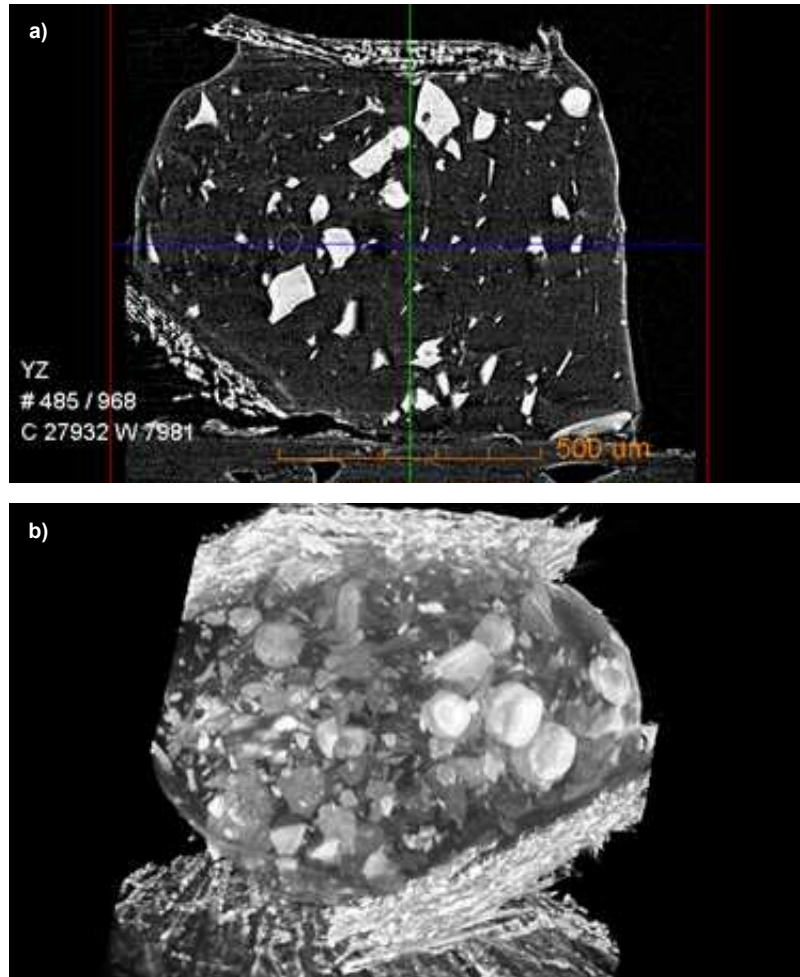


Figure S2: a) 2D slice in the reconstructed 3D volume from the x-ray μ CT scan of the composite containing particles at a volume fraction of $\phi_{nom} = 0.09$. The image is presented as given by the scanner software. b) 3D volume rendering of the reconstructed data from the x-ray μ CT scan of the composite containing particles at a volume fraction of $\phi_{nom} = 0.09$. The image is presented as given by the scanner software.

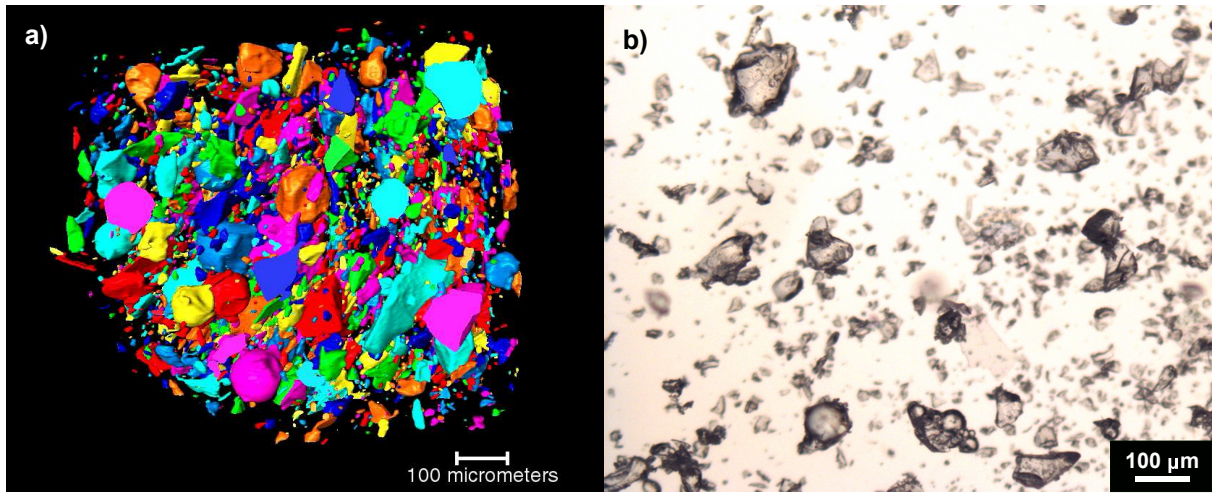


Figure S3: a) Hydrogel particles at $\phi_{nom} = 0.09$ in a soft and sticky matrix presented as a surface rendering of a segmentation of the x-ray μ CT data. b) Hydrogel particles before incorporation into the polymer matrix presented by a micrograph from optical light microscopy.

3 Rheological Measurements

Rheological measurements were carried out to evaluate the viscoelastic properties of the composites and gain information about the occurrence of particle networks. Amplitude sweeps were carried out at a frequency of 1 Hz over an amplitude range of 0.002 - 50 %. All measurements are shown in Fig. S4 a - i.

Frequency sweeps were carried out at an amplitude of 0.1 % over a frequency range of 0.0001 - 100 Hz. All measurements are shown in Fig. S4 j - r.

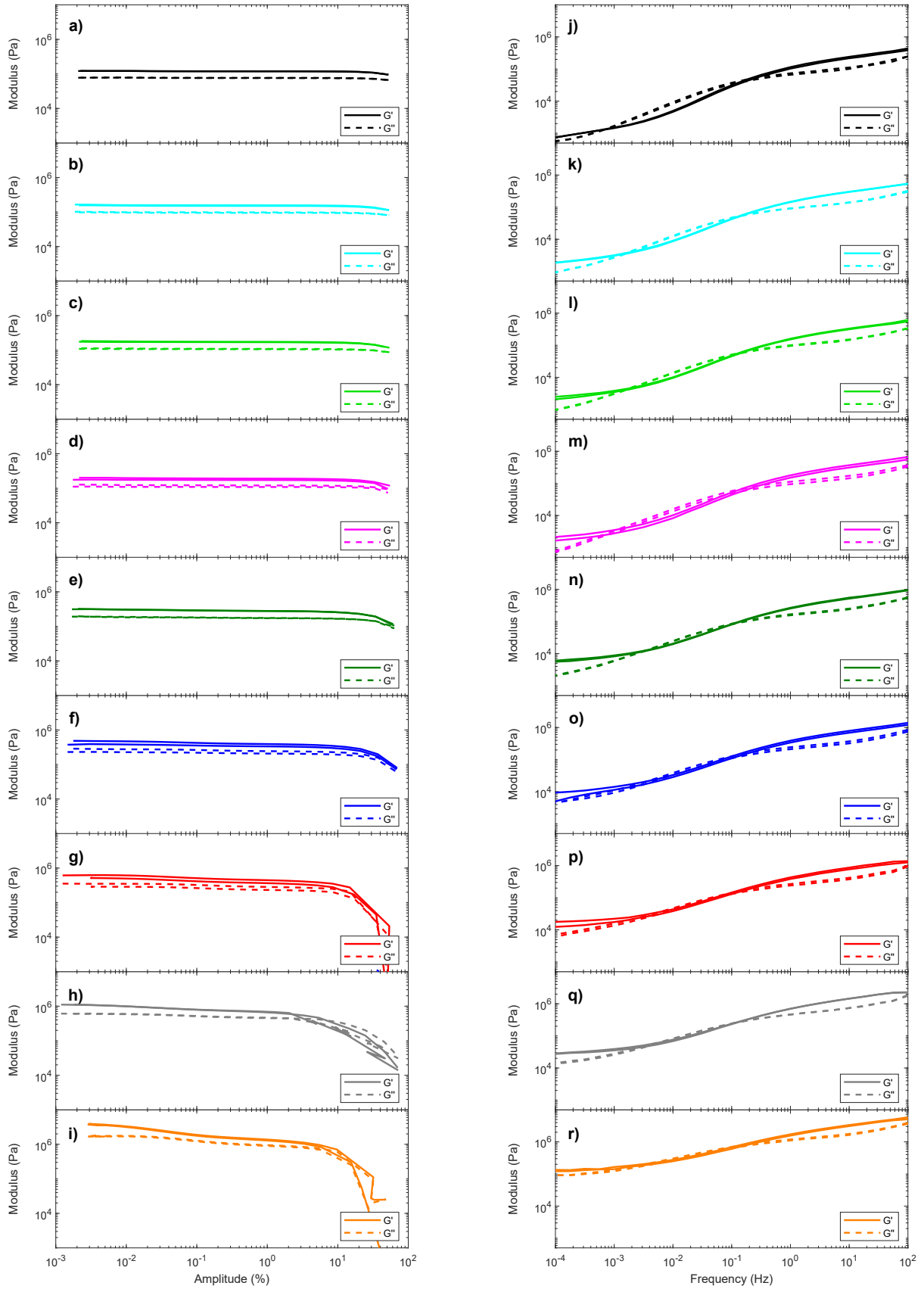


Figure S4: Amplitude sweep experiments at a frequency of 1 Hz at loadings of a) $\phi_{nom} = 0.00$, b) $\phi_{nom} = 0.06$, c) $\phi_{nom} = 0.09$, d) $\phi_{nom} = 0.12$, e) $\phi_{nom} = 0.19$, f) $\phi_{nom} = 0.27$, g) $\phi_{nom} = 0.36$, h) $\phi_{nom} = 0.46$, and i) $\phi_{nom} = 0.57$.

Frequency sweep experiments at an amplitude of 0.1 % at loadings of j) $\phi_{nom} = 0.00$, k) $\phi_{nom} = 0.06$, l) $\phi_{nom} = 0.09$, m) $\phi_{nom} = 0.12$, n) $\phi_{nom} = 0.19$, o) $\phi_{nom} = 0.27$, p) $\phi_{nom} = 0.36$, q) $\phi_{nom} = 0.46$, and r) $\phi_{nom} = 0.57$.

4 Reduced Viscosity

Suspensions of particles in polymer liquids are dominated by hydrodynamic interactions and are often evaluated in terms of their reduced viscosity, which is defined as the viscosity of the suspension divided by the viscosity of the pure polymer. There exist many empirical and semi-empirical equations to describe the development of the reduced viscosity as a function of particle loading[1]. Thereby, Le Meins et al.[2] have used the Krieger-Dougherty equation to evaluate their suspensions:

$$\eta_r = \left(1 - \frac{\phi}{\phi_{max}}\right)^{-2.5\phi_{max}} \quad (6)$$

where η_r is the reduced viscosity, ϕ is the particle loading, and ϕ_{max} is the maximum particle loading. These empirical equations are typically evaluated at moderate strain rates around 0.1 s^{-1} . In Fig. S5, the development of the reduced viscosity is shown for the composites in our study along with the predictions according to the Krieger-Dougherty equation. The data show good coincidence with the predictions, implying that the hydrodynamic interactions between the particles are responsible for the increase in the reduced viscosity.

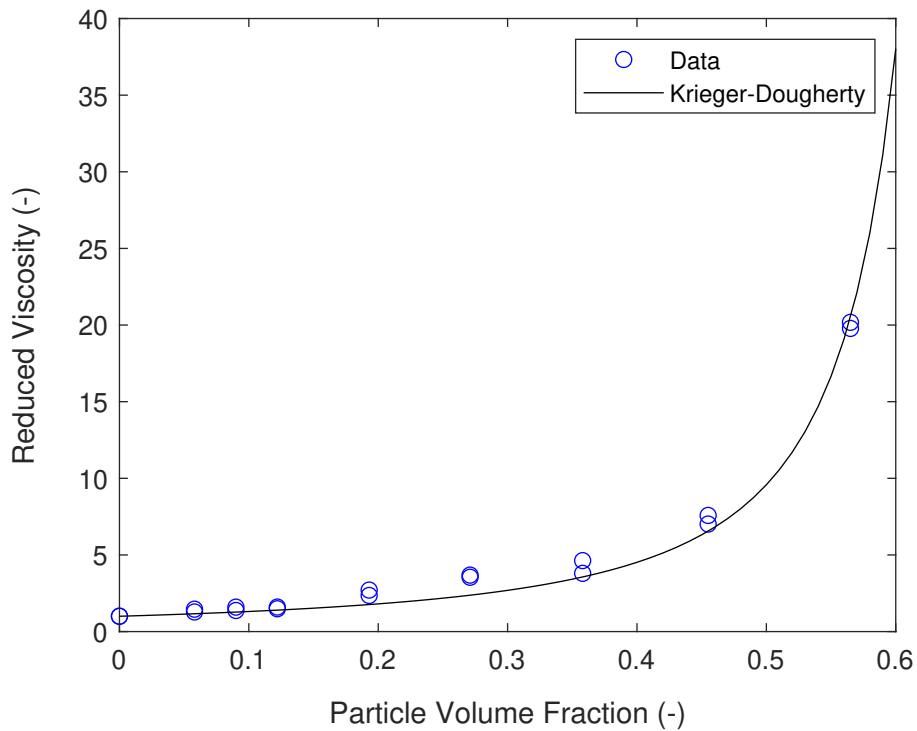


Figure S5: Development of the reduced viscosity at different particle volume fractions. The reduced viscosity has been calculated from the viscosity curves in Fig. 5 a in the manuscript at a frequency of 0.1 Hz.

5 Vapour Permeability of the Matrix

The water vapour transmission rate of the unfilled polymer matrix with a thickness of 1 mm was measured over a saturated NaCl solution (approx. 75 % RH) at 32 °C. After a lag period, during which the film was saturated, a water vapour transmission rate of 1.1×10^{-5} g/cm²/h was observed. In our experiments, if we assume that the polymer matrix is saturated instantaneously, there will be a water vapour transmission of 1.1×10^{-5} g/cm²/h (this can be regarded as the maximum rate of transmission). In Fig. S6, the cumulative transmission of water vapour through the matrix is shown along with the moisture uptake data for all composites in our study. At low particle concentrations, $\phi_{nom} = 0.06$ and $\phi_{nom} = 0.09$, the transmission through the matrix is in the order of the vapour uptake of the composites. Here, the particles are isolated and the diffusion within the particles only plays a minor role for the total diffusion. Increasing the particle loading, means that the transmission through the matrix becomes less important and diffusion through the particles is dominant.

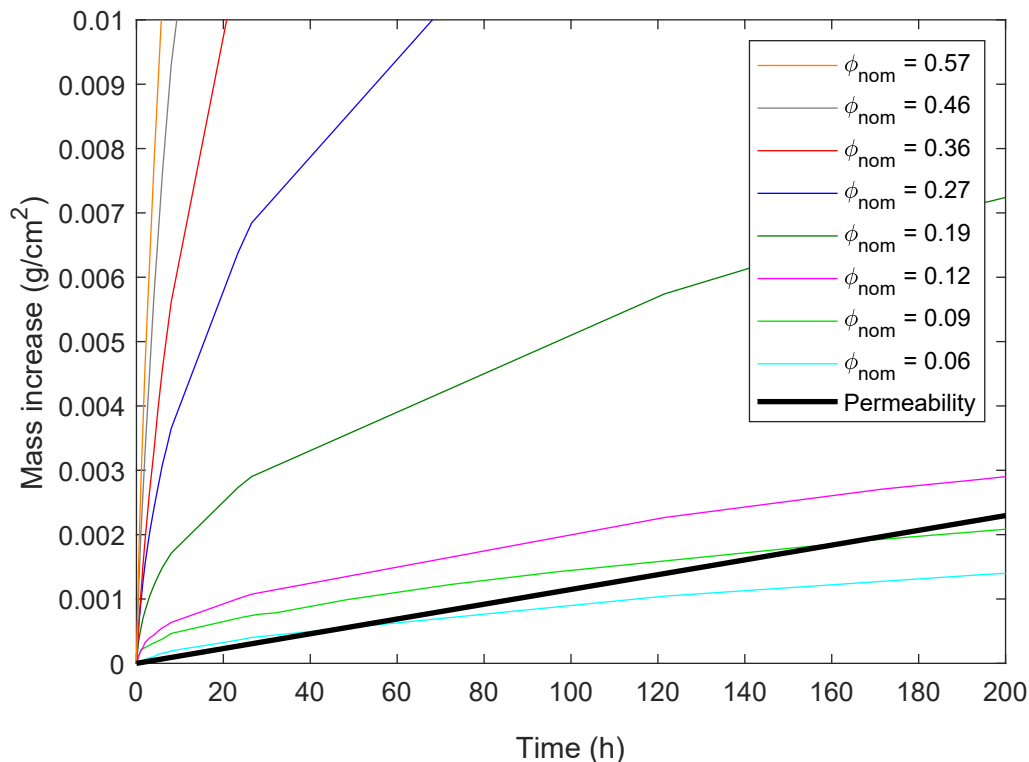


Figure S6: Water vapour uptake of the composites at 75 % RH and 32 °C. The water vapour transmission of the polymer matrix is indicated as the permeability for comparison.

References

- [1] A. B. Metzner, “Rheology of Suspensions in Polymeric Liquids,” *Journal of Rheology*, vol. 29, no. 6, pp. 739–775, 2002.
- [2] J.-F. Le Meins, P. Moldenaers, and J. Mewis, “Suspensions of monodisperse spheres in polymer melts: particle size effects in extensional flow,” *Rheologica Acta*, vol. 42, pp. 184–190, jan 2003.